Scaling methodology for buckling of composite conical shells in axial compression

Pareyns, K.; Bisagni, C.; Rudd, M.T.; Schultz, Marc R.

Publication date
2021

Document Version
Final published version

Published in
Proceedings of the American Society for Composites, Thirty-Sixth Technical Conference

Scaling Methodology for Buckling of Composite Conical Shells in Axial Compression

KAAT PAREYNS[1], CHIARA BISAGNI[1], MICHELLE T. RUDD[2] and MARC R. SCHULTZ[3]

ABSTRACT

Conical shells are commonly used as structural components for launch vehicles. The axial compression experienced during launch is one of the sizing load cases, because it can lead to loss of structural stability. Because experimentally testing these full-scale structures is cumbersome and expensive, it is expedient to understand how reduced-scale shells can be designed such that their buckling behavior is representative of the full-scale shell behavior. An analytical, sequential scaling methodology is developed based on the nondimensional governing equations for composite conical shells with a symmetric, balanced layup and negligible flexural anisotropy. Linear and nonlinear finite element analyses characterizing the buckling behavior of the different size shells yielded comparable results in terms of buckling load, meridional displacement, and buckling mode. The inclusion of geometric imperfections affects the prediction accuracy, but not to the extent that the methodology is no longer valid.

NOMENCLATURE

A_{ij}	=	membrane stiffness matrix, N/m
a_{ij}	=	membrane compliance matrix, m/N
B_{ij}	=	coupling stiffness matrix, N
D_{ij}	=	bending stiffness matrix, Nm
F	=	nondimensional stress function, -
K_1	=	nondimensional loading parameter, -
L	=	conical shell length, m
L_1, L_2	=	in-plane characteristic shell dimensions, m
m	=	number of meridional half-waves, -

[1]Delft University of Technology, Faculty of Aerospace Engineering, Kluyverweg 1, 2629 HS, The Netherlands
[2]NASA Marshall Space Flight Center, Huntsville, AL 35812, U.S.A.
[3]NASA Langley Research Center, 8 West Taylor St., MS 190, VA 23681, U.S.A.

N_1, N_2, N_{12}	=	membrane stress resultants, N/m
n	=	number of circumferential full waves, -
P	=	applied axial load, N
P_{cr}	=	critical buckling load, N
q_1, q_2	=	applied tangential surface tractions, Pa
R_1, R_2	=	radii of curvature in meridional and circumferential direction, respectively, m
R_t	=	radius at conical shell top side, m
R_b	=	radius at conical shell bottom side, m
$r(x)$	=	conical shell radius, m
$r(z_1)$	=	conical shell radius in terms of nondimensional coordinates, -
U	=	nondimensional meridional displacement, -
u	=	meridional displacement, m
V	=	nondimensional circumferential displacement, -
v	=	circumferential displacement, m
W	=	nondimensional out-of-plane displacement, -
w	=	out-of-plane displacement, m
x	=	meridional coordinate, m
y	=	circumferential coordinate, m
Z_2	=	nondimensional equivalent Batdorf-Stein parameter, -
z	=	out-of-plane coordinate, m
z_1	=	nondimensional meridional coordinate, -
z_2	=	nondimensional circumferential coordinate, -
z_3	=	nondimensional out-of-plane coordinate, -
α	=	cone angle, deg
α_b	=	nondimensional bending parameter, -
α_m	=	nondimensional membrane parameter, -
β	=	nondimensional bending orthotropy parameter, -
μ	=	nondimensional membrane orthotropy parameter, -
θ	=	ply angle, deg

INTRODUCTION

Typical launch vehicle structures are largely composed of cylindrical and conical shells. The shells are designed to withstand the primarily axial compressive loads caused by the weight of the structure and the trajectory, which can lead to buckling. As-built geometric imperfections can significantly change the load at which buckling initiates, making experimental testing imperative in characterizing the implications of these imperfections on shell stability. Launch vehicle structures can measure several meters in diameter and length, hence testing these shells often is cumbersome and expensive. Therefore, it is more feasible to test reduced-scale shells that are representative of the full-scale shells. The design of these reduced-scale shells can be obtained through a scaling methodology.

Several successful scaling methodologies have been developed for cylindrical shells. Uriol Balbin, et al. [1] set up a sequential scaling procedure for the axial buckling of sandwich cylindrical shells using nondimensional governing equations

derived by Schultz and Nemeth [2]. Rezaeepazhand and Simitses [3] studied a scaling methodology for symmetric, cross-ply laminated cylindrical shells based on the dimensional governing equations. This work was later extended by Ungbhakorn and Wattanasakulpong [4] for antisymmetric cross-ply laminated cylindrical shells. The scaling of conical shells has been investigated as well. Penning [5] reports on the scaling of the vibration characteristics of a conical stage adapter of the Saturn V. The conical shell is approximated as an equivalent cylindrical shell and is consequently scaled using a dimensional analysis. No agreement is found between the experimental results of conical shells and the equivalent cylindrical shell and it is concluded that the conical shell undergoes complex vibrations. Jiang, et al. [6] investigated the scaling of isotropic conical shells subject to impact loading with a dimensional analysis. Due to damage and plasticity, deviations from the behavior predicted by the applied scaling laws is observed. Sleight, et al. [7] compared the imperfection sensitivity of axially compressed full-height and half-height sandwich conical shells. The buckling load and imperfection sensitivity is similar for the two cases. As the circumferential size and the load magnitude are identical for the full-height and half-height shells, the complexity of testing is not reduced in this approach.

In the research presented herein, a scaling methodology for the axial buckling behavior of composite conical shells is developed using nondimensional governing equations. The use of nondimensional equations is preferred because the coefficients of the equations can be used directly as scaling parameters, and the nondimensional framework allows shells of different size to be directly compared to each other. In this paper, the setup of the scaling methodology using the governing equations is described first. Discussed next is the scaling methodology applied to a full-scale conical shell, after which the prediction is evaluated.

SCALING METHODOLOGY

The scaling methodology is developed for composite conical shells. A curvilinear coordinate system (x, y, z) is adopted, as shown in Figure 1, coincident with the surface coordinates. The corresponding displacements are u, v, and w, respectively. The conical shell has a cone angle, α, meridional length, L, and radius, $r(x)$, varying from R_t at the top side to R_b at the bottom side according to

$$r(x) = R_t + x \sin \alpha \tag{1}$$

The scaling methodology is based on nondimensional equations governing the buckling behavior of conical shells. Nemeth [8,9] developed a nondimensional framework for the buckling of laminated general shells using the Donnell-Mushtari-Vlasov theory [10]. The Kirchhoff hypothesis is imposed and it is assumed that the shell is thin-walled, meaning the thickness is small compared to the in-plane dimensions (i.e., the radius and the length). In the equations, the presence of imperfections is not presented. The nondimensionalization procedure makes each variable dimensionless, aims to minimize the number of independent parameters describing the behavior, and avoids the introduction of a direction of preference in the equations [8].

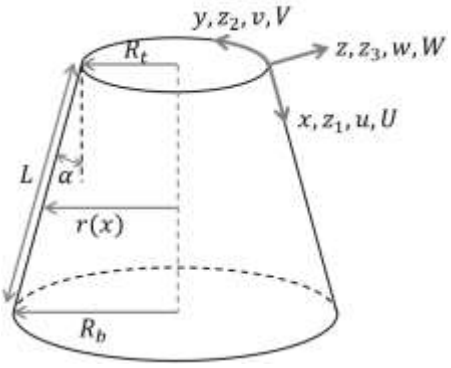

Figure 1. Geometry and coordinate system of composite conical shell.

In this study, the equations are made specific for an axially loaded conical shell with a symmetric, balanced layup and negligible flexural anisotropy. This simplification is achieved through the following substitutions in the equations of reference [8]. In accordance with the laminate assumptions, $A_{16} = A_{26} = D_{16} = D_{26} = B_{ij} = 0$, where A_{ij}, D_{ij}, and B_{ij} are the laminate stiffnesses. The characteristic dimensions are given by $L_1 = L$ and $L_2 = r(x)$, such that the in-plane coordinates can be made nondimensional as $x = L\, z_1$ and $y = r(x)\, z_2$. Substitution of these coordinates in Eq. 1 allows expression of the radius in terms of the nondimensional coordinate z_1. The corresponding radii of curvature are given by $R_1 \to \infty$ and $R_2 = \frac{r(x)}{\cos\alpha}$. Only axial compression is considered, such that, in combination with the assumed membrane prebuckling state, $N_2 = N_{12} = q_1 = q_2 = 0$, where N_2 and N_{12} are the prebuckling membrane stress resultants and q_1 and q_2 are the applied tangential surface tractions. The linearized nondimensional governing equations are consequently given as the equilibrium equation,

$$\alpha_b^2 \frac{\partial^4 W}{\partial z_1^4} + 2\beta \frac{\partial^4 W}{\partial z_1^2 \partial z_2^2} + \frac{1}{\alpha_b^2}\frac{\partial^4 W}{\partial z_2^4} + \sqrt{12} Z_2 \frac{\partial^2 F}{\partial z_1^2} - K_1 \frac{\partial^2 W}{\partial z_1^2} = 0 \tag{2}$$

and the compatibility equation,

$$\alpha_m^2 \frac{\partial^4 F}{\partial z_1^4} + 2\mu \frac{\partial^4 F}{\partial z_1^2 \partial z_2^2} + \frac{1}{\alpha_m^2}\frac{\partial^4 F}{\partial z_2^4} = \sqrt{12} Z_2 \frac{\partial^2 W}{\partial z_1^2} \tag{3}$$

where $\mu, \beta, \alpha_m, \alpha_b, Z_2$, and K_1 are nondimensional parameters defined by Eq. (4) to Eq. (9), W is the nondimensional out-of-plane displacement, and F the nondimensional stress function. Nondimensional coefficients μ and β are the membrane and bending orthotropy parameters, respectively, and depend on the membrane compliances a_{ij} and the bending stiffnesses D_{ij}. They are given by

$$\mu = \frac{2a_{12} + a_{66}}{2\sqrt{a_{11}a_{22}}} \tag{4}$$

$$\beta = \frac{D_{12} + 2D_{66}}{\sqrt{D_{11}D_{22}}} \tag{5}$$

The membrane parameter α_m and the bending parameter α_b depend on the radius-to-length ratio and the membrane compliance and bending stiffness. More specifically,

$$\alpha_m = \frac{r(z_1)}{L}\left(\frac{a_{22}}{a_{11}}\right)^{0.25} \tag{6}$$

$$\alpha_b = \frac{r(z_1)}{L}\left(\frac{D_{11}}{D_{22}}\right)^{0.25} \tag{7}$$

The equivalent Batdorf-Stein parameter Z_2 is a curvature parameter given by

$$Z_2 = \frac{r(z_1)\cos\alpha}{\sqrt{12}(a_{11}a_{22}D_{11}D_{22})^{0.25}} \tag{8}$$

Finally, the loading parameter K_1 is given by

$$K_1 = \frac{N_1\, r^2(z_1)}{\sqrt{D_{11}D_{22}}} = \frac{P\, r(z_1)}{2\pi\cos\alpha\sqrt{D_{11}D_{22}}} \tag{9}$$

where N_1 is the meridional load per unit length and P is the applied axial load.

If the governing equations (Eq. (2) and Eq. (3)) are identical for two or more conical shells, then it is expected that their buckling behavior is also identical. This logically requires that the nondimensional coefficients, given in Eq. (4) to Eq. (9), should be identical for the conical shells. Therefore, these coefficients are used as scaling parameters to determine representative reduced-scale conical shells for a given full-scale conical shell. Note that some coefficients are a function of the radius $r(z_1)$, such that they vary along the conical shell length. In order to have the parameters equal to the full-scale values for all meridional positions, they should be matched at two locations due to the linear dependency. These parameters are consequently made identical to the full-scale values at the top and bottom of the shell, namely at $z_1 = 0$ and at $z_1 = 1$. As a result, each of these coefficients that are a function of the radius give rise to two scaling parameters.

A sequential scaling methodology is set up to design reduced-scale conical shells as follows. First, the reduced-scale shell is chosen to be made of the same material as the full-scale shell and the stacking sequence of the reduced-scale shell is determined using μ and β (Eq. (4) and Eq. (5)), as these parameters only depend on material and stacking sequence. Second, the small-radius-to-length ratio R_1/L is determined by matching α_m and α_b (Eq. (6) and Eq. (7)) for $z_1 = 0$. These two parameters only depend on this ratio and on the previously determined material and stacking sequence. Third, the cone angle is found also using the α_m and α_b parameters, but at $z_1 = 1$. Again, these scaling parameters only depend on previously determined properties and the cone angle. Fourth, the radius is determined using Z_2 (Eq. (8)) for $z_1 = 0$ and, similarly, the length is found using Z_2 for $z_1 = 1$. Nondimensional load K_1 (Eq. (9)) is the objective parameter: if it is equal for full-scale and reduced-scale shells, the buckling load of the full-scale shell is appropriately predicted by the reduced-scale shell. Therefore, K_1 is not used to design the reduced-scale shell, but to evaluate the prediction capability of the methodology. Note that in the first three steps of the methodology, two scaling parameters are used to determine one reduced-scale design variable. For example, in the second step, the radius-to-length ratio is determined

using α_m and α_b at $z_1 = 0$. If these two scaling parameters require a different radius-to-length ratio in order to be identical to the full-scale value, it is chosen to take the average of the two required ratios, such that the error caused by the discrepancy is spread between the two parameters. This is exemplified in the application discussed hereafter.

APPLICATION

The scaling methodology is applied to the geometry of the Universal Stage Adapter of the Space Launch System, discussed by Sleight, et al. [7]. This component has a sandwich structure, but it is here considered as a monolithic equivalent with the same theoretical buckling load as the original sandwich shell. In this example, the full-scale shell is made of IM7/8552 carbon fiber, whose properties are reported in Table I. The stacking sequence of the full-scale conical shell is $[45/90/-45/0]_{7S}$. The geometry is described in Table II.

The reduced-scale shell is designed using the methodology described above. First, a layup is found. To restrict the number of stacking sequences to be analyzed, only one variable ply angle θ is considered. In addition, the layup should be symmetric and balanced, and have negligible flexural anisotropy. Two layup types are considered, namely $[\theta/-\theta/\bar{0}]_S$ and $[\theta/-\theta]_{S^3}$. The variation of parameters μ and β with ply angle θ is visualized in Figure 2 for the two layups. For the $[\theta/-\theta/\bar{0}]_S$ layup, the orthotropy parameters are equal to the ones of the full-scale shell for $\theta = 16°$. For the $[\theta/-\theta]_{S^3}$ layup, this is the case for $\theta = 15°$ and for $\theta = 75°$. As a result, there are three potential layups for reduced-scale designs. The consequent design steps are here explained for the first reduced-scale layup (i.e., with $\theta = 16°$ for the $[\theta/-\theta/\bar{0}]_S$ layup). The radius-to-length ratio is determined next. In order to match α_m to the full-scale value, R_1/L should be 0.308. For matching α_b, the ratio should be 0.304. The average of 0.306 is consequently used. Third, a cone angle of 8° is found using α_m and α_b at $z_1 = 1$. This value is the rounded average of the cone angle required to satisfy the two parameters. Finally, the radius and length are determined using Z_2 at $z_1 = 0$ and $z_1 = 1$, respectively. A radius R_t of 0.253 m and a length L of 0.808 m are found. The corresponding radius-to-length ratio measures 0.313, which is slightly larger than the value determined with α_m and α_b.

The three reduced-scale designs are summarized in Table II. The first reduced-scale shell is small and complies with typical test equipment constraints, given by a maximum radius of 0.4 m and a maximum height of 1.0 m [1]. The other two designs are larger. The radius-to-length ratio of the third reduced-scale shell is large, which raises concerns about possible stiffening effects in the proximity of the boundary. Table III summarizes the nondimensional coefficients of the full-scale and reduced-scale shells. The discrepancies with the full-scale values are caused by rounding of dimensions and the conflicting requirements the scaling parameters pose on the reduced-scale design variables. The largest discrepancies occur for membrane orthotropy parameter μ and measure 7.6%, 5.7%, and 5.7% for the three reduced-scale shells, respectively. This is caused by using the average value of the ply angle θ satisfying parameters μ and β and rounding that average angle to an integer value.

TABLE I. MATERIAL PROPERTIES OF IM7/8552 CARBON FIBER [11].

E_{11} [MPa]	E_{22} [MPa]	ν [-]	G_{12} [MPa]	G_{13} [MPa]	G_{23} [MPa]	t_{ply} [mm]
149916	9370	0.36	5310	5310	2655	0.18

TABLE II. DIMENSIONS OF THE CONICAL SHELLS.

	Full-scale	Reduced-scale		
Layup	$[45/90/-45/0]_{7S}$	$[16/-16/\bar{0}]_S$	$[15/-15]_{S^3}$	$[75/-75]_{S^3}$
Cone angle α	15°	8°	8°	29°
Radius R_t [m]	2.91	0.253	0.816	0.924
Length L [m]	5.00	0.808	2.61	0.847

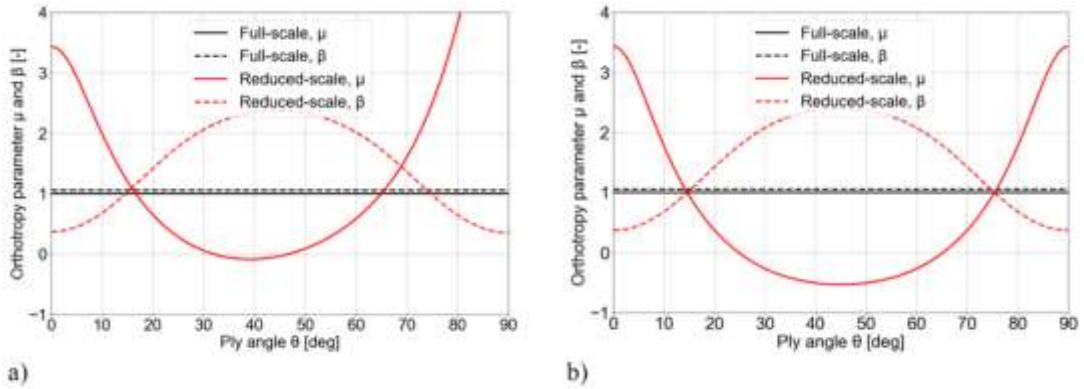

Figure 2. Ply angle vs orthotropy parameters μ and β for a) $[\theta/-\theta/\bar{0}]_S$ and b) $[\theta/-\theta]_{S^3}$.

TABLE III. NONDIMENSIONAL COEFFICIENTS OF THE CONICAL SHELLS.

		Full-scale	Reduced-scale		
		$[45/90/-45/0]_{7S}$	$[16/-16/\bar{0}]_S$	$[15/-15]_{S^3}$	$[75/-75]_{S^3}$
μ	$z_1 \epsilon [0,1]$	1.000	1.076	0.9432	0.9432
β	$z_1 \epsilon [0,1]$	1.058	1.103	1.031	1.031
α_m	$z_1 = 0$	0.5825	0.5914	0.5887	0.5800
	$z_1 = 1$	0.8413	0.8543	0.8505	0.8377
α_b	$z_1 = 0$	0.5657	0.5833	0.5887	0.5800
	$z_1 = 1$	0.8171	0.8426	0.8505	0.8377
Z_2	$z_1 = 0$	266.9	266.9	266.8	266.8
	$z_1 = 1$	385.5	385.5	385.4	385.3

BUCKLING BEHAVIOR

The buckling behavior of the full-scale and reduced-scale conical shells is analyzed to evaluate the prediction accuracy and limitations of the methodology. The analyses are performed using a semi-analytical solution and linear and nonlinear finite element analyses.

Semi-analytical Buckling Analysis

The buckling load and corresponding mode of the full-scale and reduced-scale shells are calculated using the semi-analytical solution developed by Schiffner [12] and Zhang [13] for classical orthotropic conical shells. The solution assumes a skewed buckling pattern which satisfies the boundary condition given by zero out-of-plane displacement at the edges. The results are reported in Table IV. The predicted buckling mode for all four cases has 15 meridional half-waves m and zero circumferential waves n. The nondimensional buckling load of the full-scale shell is overestimated with 1.5%, 2.9%, and 2.9% by the three reduced-scale shells, respectively. The discrepancies are caused by not satisfying all scaling parameters simultaneously due to the conflicting requirements they pose on the reduced-scale designs.

Flexural Anisotropy Effects

The governing equations for the scaling methodology are formulated for conical shells with negligible flexural anisotropy. This assumption is now verified by comparing the value of stiffness parameters D_{16} and D_{26} to the smallest of the other D_{ij} parameters. The results are given in Table V. For the first reduced-scale shell, D_{26} is larger than D_{11}, such that the flexural anisotropy cannot be considered negligible. This shell is therefore excluded from further analyses. For the full-scale shell and the other two reduced-scale shells, the values are all less than 15% so that it is reasonable to neglect the flexural anisotropy. It is observed that the flexural anisotropy assumption generally becomes better as the number of plies is increased, which results in a larger thickness. The analytically derived dimensions are also larger, such that the resulting design might not comply with typical test equipment constraints. The flexural anisotropy assumption and typical lab equipment sizes impose contradicting requirements on the reduced-scale design. The effect of the non-zero, yet negligible flexural anisotropy is analyzed further for the third reduced-scale shell using finite element analyses. The second reduced-scale shell is excluded, because it exceeds both the maximum radius and height constraints from typical lab equipment.

Finite Element Buckling Analyses

The full-scale conical shell and the third reduced-scale conical shell (i.e., with $\theta = 75°$) are analyzed with a linear eigenvalue analysis and an implicit dynamic analysis in commercial finite element software, Abaqus [14]. The shells are modelled with SC8R elements with one element through the thickness. Mesh convergence studies are carried out resulting in mesh sizes of 50 mm and 12 mm for the full-scale and the reduced-scale shell, respectively. All degrees of freedom at the shell edges are constrained, except for

TABLE IV. BUCKLING LOAD AND MODE ACCORDING TO THE SEMI-ANALYTICAL SOLUTION.

	Full-scale	Reduced-scale		
	$[45/90/-45/0]_{7S}$	$[16/-16/\bar{0}]_{S}$	$[15/-15]_{S^3}$	$[75/-75]_{S^3}$
P_{cr} [kN]	20173	103.6	1064	829.4
K_1 at $z_1 = 0$ [-]	1807	1834	1859	1859
Buckling mode (m, n)	(15,0)	(15,0)	(15,0)	(15,0)

TABLE V. BENDING-TWISTING COUPLING COMPARED TO OTHER FLEXURAL STIFFNESS VALUES, NOTE THAT $(i, j) = 1,2$.

	Full-scale	Reduced-scale		
	$[45/90/-45/0]_{7S}$	$[16/-16/\bar{0}]_{S}$	$[15/-15]_{S^3}$	$[75/-75]_{S^3}$
$\frac{D_{16}}{\min(D_{ij})}$	9.4%	38%	14%	1.5%
$\frac{D_{26}}{\min(D_{ij})}$	9.4%	153%	1.5%	14%

the axial translation direction at the top edge. The axial compression is applied to a reference point tied to the top shell edge nodes using rigid body tie constraints. For the nonlinear analysis, the compression is displacement-controlled and an eigenmode imperfection with an amplitude of 1% of the thickness is applied. The dimensional and nondimensional buckling load and displacement are reported in Table VI. The nonlinear load-displacement curve is shown in Figure 3. The nondimensional meridional displacement [9] is calculated as

$$U = \frac{uL}{\sqrt{a_{11}a_{22}D_{11}D_{22}}} \tag{10}$$

The linear buckling load and displacement of the full-scale shell are predicted by the reduced-scale shell with errors of +2.3% and +2.4%, respectively. Additionally, the differences in the reduced-scale prediction with respect to the full-scale buckling load and displacement predictions measure -0.9% and -1.2% for the nonlinear analysis. As a result, the nondimensional nonlinear stiffness, calculated as the ratio of the nondimensional load to nondimensional displacement, is predicted within +0.3%.

The finite element analyses take into account the flexural anisotropy, in contrast to the semi-analytical solution. That the effect of the non-zero bending-twisting coupling is small is supported by observing the similarly small errors between the full-scale and reduced-scale shells predicted from both analysis types. The nonlinear analysis considers a small imperfection, to which the full-scale and reduced-scale shell have a different sensitivity. The ratio of nonlinear to linear buckling load measures 0.90 for the full-scale shell and 0.87 for the reduced-scale shell. This difference in imperfection sensitivity explains why the nonlinear analysis underestimates the buckling load and displacement slightly, while the linear analysis overestimates it. The linear buckling modes, as visualized in Figure 4 are similar as well.

TABLE VI. LINEAR AND NONLINEAR FINITE ELEMENT RESULTS.

	Dimensional			
	Full-scale: $[45/90/-45/0]_{7S}$		Reduced-scale: $[75/-75]_{S^3}$	
	Load P [kN]	Displacement u [mm]	Load P [kN]	Displacement u [mm]
Linear	20289	8.43	829.7	4.65
Non-linear	18265	7.67	723.8	4.08
	Nondimensional			
	Full-scale: $[45/90/-45/0]_{7S}$		Reduced-scale: $[75/-75]_{S^3}$	
	Load K_1 [-]	Displacement U [-]	Load K_1 [-]	Displacement U [-]
Linear	1817	4399	1859	4505
Non-linear	1636	4006	1622	3957

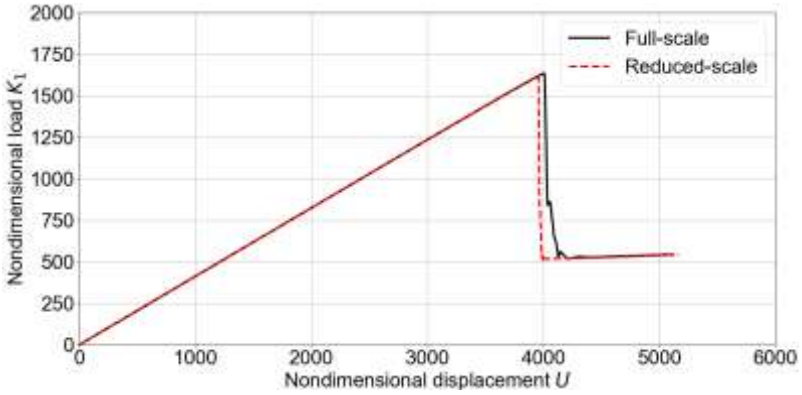

Figure 3. Nonlinear nondimensional load-displacement curves of full-scale and reduced-scale shells.

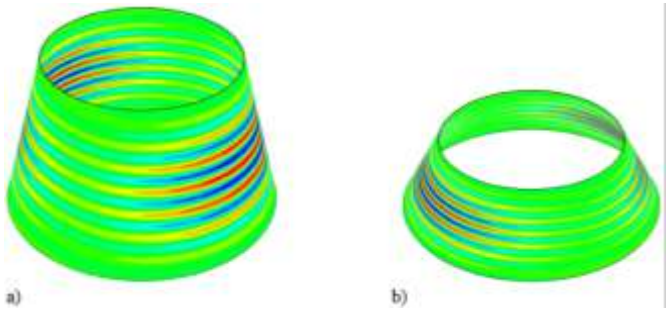

Figure 4. Linear buckling mode of a) full-scale shell and b) reduced-scale shell. The reduced-scale shell is 3x enlarged with respect to the full-scale shell for visibility purposes.

CONCLUSIONS

An analytical scaling methodology for the buckling of composite conical shells in axial compression has been developed. This methodology enables the design of representative reduced-scale shells in a specific sequential manner and the study of the buckling behavior of the full-scale shell through the behavior of a reduced-scale shell. The methodology is based on the nondimensional Donnell-Mushtari-Vlasov equations for conical shells with a symmetric, balanced layup, and negligible flexural anisotropy. The applicability of the methodology has been exemplified by the scaling

of a monolithic composite conical shell with the geometry of the Universal Stage Adapter of the Space Launch System. Three reduced-scale shells were designed, from which it was observed that the flexural anisotropy assumption and the constraints given by typical lab equipment pose conflicting requirements on the reduced-scale design. It was also observed that the inclusion of imperfections and the difference in imperfection sensitivity of the full-scale and reduced-scale shells influence the prediction. Despite this, the results obtained across all analyses for all evaluated buckling parameters showed good correlation. The applicability of the scaling methodology can be improved by including scaling parameters for the flexural anisotropy and by further investigation of the effect of imperfections. Finally, the methodology still has to be validated with experimental testing.

REFERENCES

1. Uriol Balbin, C. Bisagni, M.R. Schultz, and M.W. Hilburger. Scaling methodology applied to buckling of sandwich composite cylindrical shells. *AIAA Journal*, 58(8):3680–3689, 2020. doi:10.2514/1.J058999.
2. M.R. Schultz and M.P. Nemeth. Buckling imperfection sensitivity of axially compressed orthotropic cylinders. In *51st AIAA/ASME/ASCE/AHS/ASC Structures, Structural dynamics, and Materials Conference*. American Institute of Aeronautics and Astronautics, 2010. doi:10.2514/6.2010-2531.
3. J. Rezaeepazhand, G.J. Simitses, and J.H. Starnes. Scale models for laminated cylindrical shells subjected to axial compression. *Composite Structures*, 34(4):371–379, 1996. doi:10.1016/0263-8223(95)00154-9.
4. V. Ungbhakorn and N. Wattanasakulpong. Structural similitude and scaling laws of antisymmetric cross-ply laminated cylindrical shells for buckling and vibration experiments. *International Journal of Structural Stability and Dynamics*, 7(4):609–627, 2007. doi:10.1142/S0219455407002459.
5. F.A. Penning. Use of dynamic scale models to determine launch vehicle characteristics. Technical Report 19690031776, NASA Marshall Space Flight Center, Huntsville, Alabama, 1969.
6. P. Jiang, W. Wang, and G.J. Zhang. Size effects in the axial tearing of circular tubes during quasi-static and impact loadings. *International Journal of Impact Engineering*, 32(12):2048–2065, 2006. doi:10.1016/j.ijimpeng.2005.07.001.
7. D.W. Sleight, A. Satyanarayana, and M.R. Schultz. Buckling imperfection sensitivity of conical sandwich composite structures for launch-vehicles. In *2018 AIAA/ASCE/AHS/ASC Structures, Structural Dynamics, and Materials Conference*. American Institute of Aeronautics and Astronautics, 2018. doi:10.2514/6.2018-1696.
8. M.P. Nemeth. Nondimensional parameters and equations for buckling of symmetrically laminated thin elastic shallow shells. Technical Report 19910013084, NASA Langley Research Center, Hampton, Virginia, 1991.
9. M.P. Nemeth. Nondimensional parameters and equations for nonlinear and bifurcation analyses of thin anisotropic quasi-shallow shells. Technical Report 20100027403, NASA Langley Research Center, Hampton, Virginia, 2010.
10. D.O. Brush and B.O. Almroth. *Buckling of bars, plates, and shells*. McGraw-Hill, 1975.
11. K. Marlett, Y. Ng, and J. Tomblin. Hexcel 8552 IM7 unidirectional prepreg 190 gsm & 35%RC qualification material property data report. Technical report, National Center for Advanced Materials Performance, CAM-RP-2009-015 Rev. A, Wichita, KS, 2011.
12. K. Schiffner. *Spannungs- und Stabilitätsuntersuchungen an dünnwandigen Kegelschalen bei axialsymmetrischen Randbedingungen*. PhD dissertation, RWTH Aachen University, 1966.
13. G.Q. Zhang. *Stability analysis of anisotropic conical shells*. PhD dissertation, Delft University of Technology, 1993.
14. Dassault Systemes. *Abaqus Analysis 6.14 User's Guide*. Dassault Systemes, Providence, Rhode Island, 2016.